Dynamics of Excess Electron Localization in Liquid Helium and Neon

Michael Rosenblit and Joshua Jortner*

School of Chemistry, Tel Aviv University, Ramat Aviv, 69978 Tel Aviv, Israel

Received: August 23, 1996[⊗]

In this paper, we address the relations between the structure, electronic level structure, energetics, and localization dynamics of an excess electron in a bubble in liquid ^{4}He, ^{3}He, and Ne. Our treatment of the dynamics of formation for the electron bubble rests on a quantum mechanical Wigner−Seitz description of the excess electron in conjunction with a hydrodynamic picture for the liquid. The dynamics of electron localization is described in terms of the initial formation of an incipient bubble of radius 3.3−3.5 Å followed by adiabatic bubble expansion in the ground electronic state. The hydrodynamic model for bubble expansion considers the expansion of a spherical cavity in an incompressible liquid with the energy dissipation being due to the emission of sound waves. This model predicts the bubble expansion time (τ_b^D) in liquid ^{4}He to be $\tau_b^D = 8.5$ ps at $P = 0$, exhibiting a marked pressure dependence (decreasing by a numerical factor of 4 at $P = 16$ atm) and revealing a small isotope effect of $\tau_b^D(^4\text{He})/\tau_b^D(^3\text{He}) = 0.83$ in liquid ^{3}He, while for liquid Ne, $\tau_b^D \cong 1$ ps. The collapse times of the empty bubble formed by vertical photoionization of the electron bubble are $\tau_c = 19.8$ ps for ^{4}He and $\tau_c = 34$ ps for ^{3}He, with τ_c being considerably longer than τ_b^D, reflecting the effect of the kinetic electron energy on the fast electron bubble expansion. The interrogation of the electron bubble localization dynamics by femtosecond absorption spectroscopy is explored by the analysis of the temporal evolution of the electronic excitation energies.

I. Prologue

The elucidation of the interrelationship between the structure, electronic level structure, energetics, and dynamics in complex systems, e.g., clusters and condensed matter, constitutes a major challenge of modern chemical physics. In this context, the dynamics of excess electron localization in some macroscopic dense fluids, i.e., liquid He, Ne, H_2, and D_2, is of central interest. The interaction between an excess electron and a few-electron closed-shell atom or molecule, e.g., He, Ne, or H_2, is strongly short-range repulsive, with a weak long-range core polarization.[1−4] Accordingly, the conduction band energy (V_0) in the corresponding dense fluids is large and positive, being located above the vacuum level; i.e., V_0(calc) = 1.02 eV[4−9] and V_0(expt) = 1.05 ± 0.05 eV[10−13] for liquid ^{4}He, V_0(calc) = 0.9 eV[4,14,15] and V_0(expt) = 1.0 ± 0.2 eV[16,17] for liquid ^{3}He, V_0(calc) = 0.45 eV[14,15] and V_0(expt) = 0.67 ± 0.05 eV[14,15,18] for liquid Ne, and V_0(calc) = 1.25 eV[4,14,15] and V_0(expt) > 2 eV[18] for liquid H_2 (where calc and expt denote calculated and experimental data, respectively). Consequently, the energetic instability of the conduction band quasifree excess electron state in these liquids induces the formation of a localized "electron bubble" state, with the electron being confined to a cavity whose total energy is located below the conduction band. Excess electron localization, accompanied by large configurational changes, prevails in liquid ^{4}He,[4,5,8−13,19−26] in ^{3}He,[4,5,26] H_2 and D_2,[4] and Ne,[4,20] and also presumably in some large finite systems, e.g., internal excess electron localization in large clusters of ^{4}He.[27,28] Extensive theoretical[5,20−26] and experimental[19,22,24,26] studies provided a coherent physical picture of the structure, energetics, electronic level structure, and spectroscopy of the electron bubble in liquid helium, which involve its energetic stability,[5,11,20,26] its radius,[5,20−23] its compressibility,[21] the "critical" density for the electron localization in dense He gas,[5] electron localization in solid helium,[29] the energetics,[23−25] and the line broadening[24,25] of the bound−bound electronic transitions and the photoionization threshold.[22,23] The relation between these attributes and dynamics was not yet established.

Of considerable interest is the dynamics of excess electron localization in dense fluids consisting of few-electron constituents and characterized by $V_0 > 0$. This issue pertains to the dynamics of electron localization accompanied by large configurational changes in the fluid. Experimental information is scarce. Experiments on positronium annihilation in liquid He and their theoretical interpretation[30,31] reveal that the localized positronium bubble is formed on a time scale which is short relative to the lifetime of the orthopositronium; i.e., $\tau > 100$ ps. On the other hand, Muon spin relaxation experiments via the formation of Muonium in liquid neon reveal that part of the excess electrons localize fast within less than 10^3 ps, while another fraction does not localize on the 10^3-ps time scale.[32] Experimental information on the time scale of the relaxation of a quasifree electron to form the electron bubble in liquid helium emerged from the electron injection experiments of Hernandez and Silver,[33,34] which indicated that an energetic (∼1-eV) electron relaxes to a bubble state within a time of $\tau \sim 2$ ps. Jiang et al.[27] provided a rough estimate of the characteristic time for bubble formation in liquid He in terms of $\tau \sim R_b/C_s$, where $R_b = 17$ Å is the bubble radius and $C_s = 240$ ms^{-1} is the speed of the sound, resulting in $\tau \sim 7$ ps. On the theoretical front, an early study[35] proposed the incipient electron bubble formation in liquid He via the nonradiative electron localization process originating from nonadiabatic crossing of the nuclear potential energy surfaces of the quasifree and localized excess electron states. Recently, this process was treated by the semiclassical surface hopping trajectory method calculations,[36] which provided a time scale of 0.2−0.3 ps for electron cavity formation in high density ($\rho^* = 0.9$) He gas at $T = 309$ K. Subsequently, the incipient bubble is expected to expand to form the configurationally relaxed electron cavity (e.g., cavity radius $R_b \cong 17$ Å in liquid ^{4}He at zero pressure and $T = 0.4$ K[5,20−23]).

We addressed[37] the time-resolved dynamics of the electron bubble formation in liquid He, considering the adiabatic process

[⊗] Abstract published in *Advance ACS Abstracts,* December 15, 1996.

S1089-5639(96)02625-4 CCC: $14.00

TABLE 1: Surface Tension (γ), Density (ρ), and Dielectric Constant (ϵ), Together with the Calculated Energy of the Bottom of the Conduction Band (V_0), the Equilibrium Radius (R_b) of the Localized Electron Bubble, and the Radius (R_0) of the Incipient Bubble

	T, K	γ, dyn/cm	ρ, Å−3	ϵ	V_0, eV	R_0, Å	R_b, Å
^{4}He	0.4	0.36[a,b]	0.0218[c,d]	1.0588	1.02	3.5	17.0
	3.2	0.18[a,b]	0.021[c,d]				
	4.0	0.12[a,b]	0.0195[c,d]				
^{3}He	0.4	0.16[e,f]	0.0167[g]	1.0428	0.9	3.7	19.0
	3.2	0.02[e,f]	0.012[g]				
Ne	25	5.5[h]	0.037[i]	1.51	0.62	3.3	7.5

[a] Reference 56. [b] Reference 57. [c] Reference 58. [d] Reference 59. [e] References 3 and 12. [f] Reference 60. [g] Reference 61. [h] Reference 62. [i] Reference 63.

where the strongly repulsive electron−helium interaction drives out a large number of atoms toward regions where the electron density is low, while the electron is localized within the fluid dilation where the helium density is negligible. The electron bubble dynamics was described by a hydrodynamic model for cavity expansion. This hydrodynamic model constitutes the reverse situation of the Rayleigh model[38] for cavity collapse in a liquid induced by external pressure. The Rayleigh model[38] for cavity collapse was recently advanced by Rips[39] for the description of the solvation dynamics of the solvated electron in water, where cavity contraction in the polar liquid is induced by long-range attractive polarization (large polaron) interactions. Recently, it came to our attention[40] that Khrapak and his colleagues also considered positronium and electron bubble relaxation using hydrodynamic models.[41−43] Our study[37] of the dynamics of electron bubble formation in liquid He rested on the combination of a quantum mechanical picture for the excess electron in conjunction with a hydrodynamic model for the fluid expansion. In our preliminary report, the liquid was described as an incompressible fluid devoid of energy dissipation, with the expansion time (τ_b) for the attainment of the equilibrium cavity Radius (R_b) being taken as the first passage time.[37] These calculations[37] provided a lower limit for τ_b. Our analysis of the electron bubble dynamics was extended to account for energy dissipation in the cavity expansion, which constitutes the subject matter of this paper. Energy dissipation in the bubble expansion is associated with viscosity effects and emission of sound waves, which drives the system toward equilibrium, with the sound wave emission mechanism[44] constituting the dominating dissipative process. We report on the application of the hydrodynamic model with dissipation for the electron bubble dynamics in liquid ^{4}He, ^{3}He, and Ne. The results of our calculations for the electron bubble dynamics in liquid helium will be supplemented by the calculations of time-resolved electronic spectra, making contact with experimental reality.

II. Potential Energy Surfaces

We consider the decay of the delocalized, energetically unstable quasifree electron into the localized electron bubble state in its ground electronic state. The adiabatic potential energy surfaces[20,35,37] for the ground (1s) localized electronic state and for the quasifree excess electron state can be obtained from the Wigner−Seitz (WS)[4,5,21] model for the corresponding electronic energies and from a continuum model for the bubble energy. The electronic energy (V_0) of the quasifree electron state is

$$V_0 = \hbar^2 k_0^2/2m + 2\pi\rho a\hbar^2/m - (8\pi^2/3)\alpha e^2\rho^{4/3}F \quad \text{(II.1)}$$

where ρ is the solvent density, α is the atomic polarizability, $a = 0.01$ Å is the single atom polarizability scattering length,[6,7] $F = [1 + 8\pi\alpha\rho/3]^{-1}$ is the screening factor,[4] and k_0 is obtained from the WS condition.[4,21] The electronic energy of the ground state, $E_e^{1s}(R)$ (for a cavity radius, R), was obtained by the procedure of Springett et al.,[4,21] with

$$E_e^{1s}(R) = (\hbar\kappa X)^2/2m \qquad \kappa = (2mV_0/\hbar^2)^{1/2} \quad \text{(II.2)}$$

and X being obtained from the boundary condition

$$\text{cotg}(X\kappa R) = -(1 - X^2)^{1/2}/X \quad \text{(II.2a)}$$

The electronic energies of electronically excited localized states, e.g., 1s, 2s, 2p, ..., were calculated by a numerical integration of the equations of Springett et al.[4] for a particle in a spherical well. The potential energy surfaces are presented in terms of the cavity radius (R) dependence of the total energy of each electronic state. The total energy of the quasifree electron state is

$$\bar{V}_0(R) = V_0 + E_b(R) \quad \text{(II.3)}$$

with V_0 being given by eq II.1, while the total energy of the ground localized electronic state is

$$E_t^{1s}(R) = E_e^{1s}(R) + E_b(R) + E_p(R) \quad \text{(II.4)}$$

The bubble energy, $E_b(R)$, in eqs II.3 and II.4 is[4,5,8−13,19−26]

$$E_b(R) = 4\pi R^2\gamma + (4\pi/3)PR^3 \quad \text{(II.5)}$$

where γ is the surface tension and P the external pressure (Table 1) and

$$E_p(RP) = -(e^2/2R)(1 - 1/\epsilon)$$

is the electronic polarization energy and ϵ is the dielectric constant (Table 1).

We shall be interested in the energetics and dynamics of the electron bubble in liquid He over a broad pressure range (P = 0−20 atm). Experimental data for the pressure dependence of γ are not yet available. The Amit and Gross[45] theory predicts that γ increases by a numerical factor of ∼2 in the pressure range 0−25 atm. Hernandez and Silver[33] suggested that γ increases by about 35% in the pressure interval 0−20 atm. For the analysis of the spectroscopy of the electron bubble in liquid helium, Grimes and Adams took $\gamma = 0.341$ dyn/cm,[24] and Golov took $\gamma = 0.354$ dyn/cm,[46] being independent of pressure. Shin and Woo[47] used a weak pressure dependence of $\gamma = 0.39$ dyn/cm for $P = 0$ atm and $\gamma = 0.41$ dyn/cm for $P = 16.8$ atm, whereas Miyakawa and Dexter,[23] Fowler and Dexter,[20] and Springett et al.[21] assumed that γ varied with P according to the theory of Amit and Gross.[45] This procedure accounts reasonably well for the pressure dependence of R_b. In our calculations, we used the Amit and Gross[45] theory for the pressure dependence of surface tension.

The equilibrium electron cavity radius (R_b) is obtained from the minimization of $E_t^{1s}(R)$ (Table 1). The potential energy surfaces for the excess electron in liquid ^{4}He at $P = 0$ are portrayed in Figure 1. The crossing of the potential energy surfaces for the quasifree electron state, $\bar{V}_0(R)$, and the localized ground state, E_t^{1s}(R), is exhibited when

$$E_e^{1s}(R) = V_0 \quad \text{(II.6)}$$

Condition II.6 is realized (at $P = 0$) for the cavity radius R_0 = 3.5 Å. This value of R_0 constitutes the incipient cavity radius

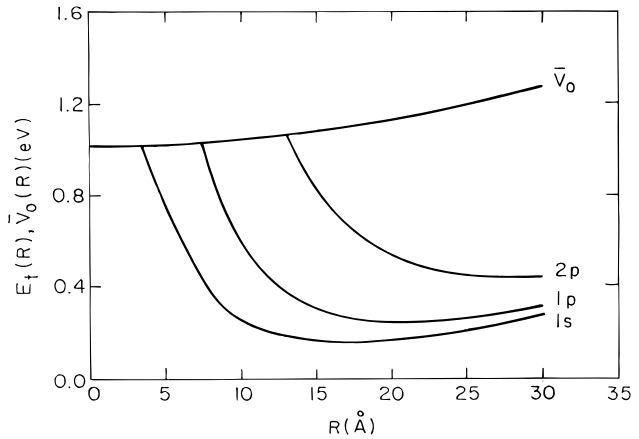

Figure 1. Configurational diagrams for the ground electronic state $E_t^{1s}(R)$, for the bound excited electronic states $E_t^{1p}(R)$ and $E_t^{2p}(R)$, and for the quasifree electron state $\bar{V}_0(R) = V_0 + E_b(R)$ in liquid He at $P = 0$.

for electron localization. R_0 is comparable to the lower limit $R_>$ of the cavity radius for the attainment of a localized state. A simple model[4,12] implies that $\pi/2 \leq X\kappa R_>$, resulting in $R_> = 3.0$ Å (at $P = 0$). A more elaborate treatment of the energetics of electron localization on the basis of the Springett−Cohen−Jortner model[4,21] implies that only a delocalized state of the excess electron exists for $X > 0.97$; the metastable bubble can be formed in the range

$$0.85 \leq X \leq 0.97$$

$$1.87 \leq \kappa R \leq 2.5 \qquad \text{(II.7)}$$

while the energetically stable bubble is formed in the region $X \leq 0.85$, $\kappa R \geq 2.5$. Thus, the onset of the formation of the metastable localized bubble is realized according to eq II.7 for $R_> = 3.46$ Å (at $P = 0$). Electron polarization effects, which were not included in eq II.7, will result in a slight decrease of $R_>$. From this analysis, we conclude that $R_0 \gtrsim R_>$. Our value of the incipient bubble radius $R_0 = 3.5$ Å is in reasonable agreement with the experimental estimate of Hernandez and Silver,[33,34] $R_0 \sim 4$ Å.

III. Electron Bubble Dynamics

(III.A) Dynamic Model. We shall consider the time evolution of the electron bubble in terms of an adiabatic process of the cavity expansion from R_0 to the equilibrium radius R_b (Table 1). Concurrently, we shall also consider time scales for the collapse of an empty bubble formed by photoionization of the ground excess electron state. Energy dissipation during the electron bubble expansion and of the empty bubble collapse will be characterized by the emission of sound waves.

We describe the dynamic of the electron bubble formation on the basis of the following assumptions:

(1) The initial electron localization in the incipient bubble of radius R_0 is fast on the time scale of the equilibrium bubble formation. Initial electron localization in high-density He gas at 309 K treated by surface-hopping calculations[36] occurs on the time scale of 50−100 fs, providing an a posteriori justification for this assumption.

(2) The equilibrium configuration of the bubble, which is characterized by radius R_b, is reached by its expansion, with the spherical shape being retained during the expansion process.

(3) The bubble radius, R, is the reaction coordinate for the adiabatic process.

(4) The liquid helium is described as an incompressible continuum.

The cavity expansion time, $\tau(R)$, from the initial cavity radius, R_0, to a radius R ($\leq R_b$) is given by the first passage time

$$\tau(R) = \int_{R_0}^{R} dR'/V(R') \qquad \text{(III.1)}$$

where $V(R')$ is the velocity of the cavity boundary. $V(R')$ is determined by the electronic energy, the bubble energy, the liquid density, and the energy dissipation. The expression for $\tau(R)$, eq III.1, is isomorphous to the description of the dynamics of ultrafast molecular processes, i.e., molecular dissociation[48] and Coulomb explosion,[49] whose time scales are described by sliding on a repulsive molecular potential surface. We have thus provided a unified description of molecular (dissociative) dynamics and (electron bubble) dynamics in the condensed phase.

(III.B) Incompressible Liquid in the Absence of Dissipation. In our previous work,[37] we have considered electron cavity dynamics in an incompressible liquid in the absence of energy dissipation. Within the framework of this simple model, the electron bubble expansion time (τ_b) for the attainment of the equilibrium radius (R_b) is taken to be represented by the first passage time at $R = R_b$. The incompressibility of the liquid implies the continuity condition $r^2 v(r) = R^2 V(R)$ so that the kinetic energy (K) of the liquid is

$$K(R) = (\rho/2)\int_R^\infty dr\, 4\pi r^2 [v(r)]^2 = 2\pi\rho[V(R)]^2 R^3 \qquad \text{(III.2)}$$

In the absence of energy dissipation, energy conservation implies that the kinetic energy of the liquid is equal to the total change of the free energy, $\Delta F(R)$, of the bubble expansion process

$$K(R) = \Delta F(R) = \bar{V}_0(R_0) - E_t^{ls}(R) \qquad \text{(III.3)}$$

Equations III.1−III.3 result in

$$V(R) = (2\pi\rho R^3)^{-1/2}[\bar{V}_0(R_0) - E_t^{1s}(R)] \qquad \text{(III.4)}$$

and

$$\tau(R) = (2\pi\rho)^{1/2}\int_{R_0}^{R} dR' (R')^{3/2} [\bar{V}_0(R_0) - E_t^{1s}(R')]^{-1/2} \qquad \text{(III.5)}$$

The expansion time for the attainment of the equilibrium bubble radius (i.e., $R = R_b$) is $\tau_b = \tau(R_b)$.

In Table 2, we present the results of the model calculations for τ_b in liquid ^{4}He, ^{3}He, and Ne. The data for ^{4}He and for ^{3}He exhibit an isotope effect $\tau_b(^4\text{He})/\tau_b(^3\text{He}) = 0.83$, correcting the value of 0.97 previously reported by us.[37] The electron bubble expansion time in liquid Ne ($R_b = 7.5$ Å) is considerably shorter than in liquid He ($R_b = 17$ Å), mainly due to the lower value of R_b. We shall return to these issues in section IV, after considering energy dissipation effects.

A cursory examination of the cavity boundary velocity, $V(R)$, for liquid He in the absence of energy dissipation (Figure 2) calculated from eq III.4 reveals that over a broad R domain, $V(R)$ exceeds the velocity of sound $C_s = 240$ cm s^{-1}. This feature is inconsistent with the incompressible continuum description of the fluid.[44] Furthermore, in the model incompressible fluid, the turning point (at $R = R_T$) for the electron cavity will be exhibited at $R_T = 60$ Å (Figure 2), which is considerably larger than R_b. The first passage time description adopted[37] for the electron bubble dynamics implicitly assumes that energy dissipation is effective, reducing $V(R)$ and drastically reducing the value of R_T for the turning point, bringing R_T close

TABLE 2: Expansion Times for the Attainment of the Equilibrium Radius of the Electron Bubble in ^{4}He, ^{3}He, and Ne[a]

	T, K	*P*, atm	τ_b, ps	τ_b^D, ps
^{4}He	0.4	0	3.9	8.5
^{4}He	3.2	1.0	3.7	4.7
^{3}He	0.4	0	4.7	10.2
^{3}He	3.2	1.0	3.9	5.8
Ne	25	1.0	0.55	1.1

[a] τ_b was calculated for the incompressible liquid in the absence of energy dissipation, while τ_b^D includes the effects of energy dissipation due to sound emission.

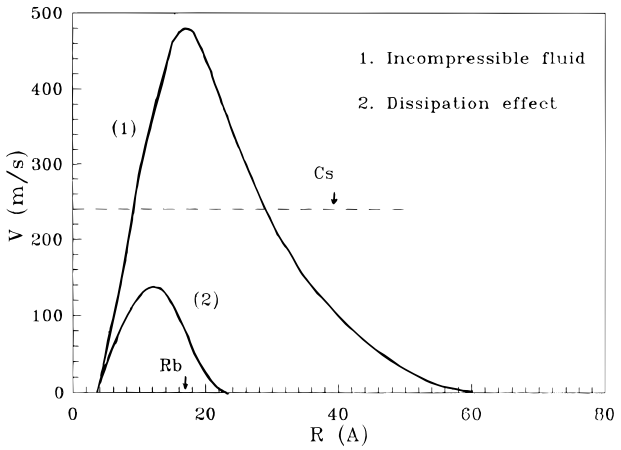

Figure 2. *R* dependence of the velocity $V(R)$ of the electron cavity boundary in liquid ^{4}He at $P = 0$ ($T = 0.4$ K). (1) Incompressible fluid in the absence of energy dissipation. (2) Incompressible fluid with dissipation due to sound emission. The equilibrium cavity radius is marked by R_b. C_s represents the velocity of sound in liquid ^{4}He.

to R_b. These expectations are indeed borne out by the analysis of energy dissipation effects.

(III.C) Energy Dissipation via Sound Emission. We consider energy dissipation during the electron cavity expansion in monoatomic liquids due to sound emission. This problem was recently studied by Rips[39] in the context of electron solvation in water. The calculation of the energy dissipation rate will be based on the assumption that the wavelength of the sound waves is longer than the characteristic radius of the cavity; i.e., $\lambda \gg R_b$. In this case, the dynamics of the fluid in the vicinity of the cavity can be described in terms of the potential flow of incompressible liquid. Far away from the cavity, it can be described in terms of the sound waves propagation. We shall express the rate of energy emission in the form of sound waves using the standard analysis[44] for the oscillation in the size of the electron cavity

$$I = (\rho/4\pi C_s)\langle \ddot{V}(t - r/C_s)]\rangle \quad \text{(III.6)}$$

where C_s is the sound velocity, V is the volume of the cavity, and the angular brckets denote averaging over the period of the cavity oscillation. The second time derivative of the volume can be expressed in the form

$$\ddot{V} = 4\pi(2RV^2 + R^2\dot{V}) \quad \text{(III.7)}$$

Here R is the radius of the cavity, while V and $\dot{V}$ are the velocity and the acceleration of the cavity boundary

$$V = (2\pi\rho)^{-1/2}R^{-3/2}(V_0 - E_t^{1s}(R))^{1/2} \quad \text{(III.8)}$$

$$\dot{V} = (1/4\pi\rho R^4)(3(E_t^{1s}(R) - V_0) - R\partial E_t(R)/\partial R) \quad \text{(III.9)}$$

Equations III.6−III.9 result in

$$I = (1/4\pi\rho C_s)\langle 1/R^4[V_0 - E_t^{1s}(R) - R\partial E_t^{1s}(R)/\partial R]^2\rangle \quad \text{(III.10)}$$

The total energy dissipated in the form of the sound waves (ΔE_D^{SE}) upon cavity expansion from the initial size to the radius R is

$$\Delta E_D^{SE}(R) \cong I\tau(R) \quad \text{(III.11)}$$

where $\tau(R)$ is the cavity expansion time evaluated neglecting the dissipation (section III.B). We write the energy dissipation in the form

$$\Delta E_D^{SE}(R) \cong (\tau(R)/4\pi\rho C_s)\langle 1/R^4[(V_0 - E_t^{1s}) - R\partial E_t^{1s}(R)/\partial R]^2\rangle \quad \text{(III.12)}$$

After simple transformation, it takes the form

$$\Delta E_D^{SE}(R) \cong (\tau(R)/4\pi\rho C_s)\langle 1/R^4[(V_0 + E_e^{1s}) - 12\pi R^2\gamma - 16\pi PR^3/3]^2\rangle \quad \text{(III.13)}$$

The averging of the sound dissipation rate in eq III.13 has to be performed in a self-consistent manner over the interval from R_0 to the genuine turning point R_T, which is determined by dissipation effects. In the calculations reported herein, we have calculated $\Delta E_D^{SE}(R)$ by averaging the dissipation rate over the range R_0 to $R_T = 23$ Å, which corresponds to the turning point when energy dissipation is operative. We find that other averaging procedures change the final value the cavity expansion time by less than 10%.

The cavity boundary velocity corrected for the dissipation, $V_D(R)$, is given by incorporating energy dissipation, eq III.13, in eqs III.4 and III.5, resulting in

$$V_D(R) = (2\pi\rho R^3)^{-1/2}[\bar{V}_0 - E_t^{1s}(R) - \Delta E_D^{SE}(R)]^{1/2} \quad \text{(III.14)}$$

and the electron bubble expansion time (for $R = R_b$) can now be expressed in the form

$$\tau_b^D = (2\pi\rho)^{1/2}\int_{R_0}^{R_b} dR R^{3/2}[\bar{V}_0 - E_t(R) - \Delta E_D^{SE}(R)]^{-1/2} \quad \text{(III.15)}$$

The bubble expansion velocity of the electron bubble, calculated from eq III.14 and portrayed in Figure 2, markedly decreases due to dissipation effects. Furthermore, the effects of energy dissipation drastically reduce the turning point for the electron cavity expansion from $R_T = 60$ Å in the abesence of dissipation to $R_T = 23$ Å due to sound emission. Now $V(R)$ for all R falls below the value of the sound velocity, rendering the incompressible continuum description of the fluid adequate.

IV. Electron Bubble Expansion Times

In Table 2, we present typical data for the electron bubble expansion times (τ_b^D) in liquid ^{4}He, ^{3}He, and Ne, calculated incorporating energy dissipation. From the comparison of the values of τ_b^D with the values of τ_b (without sound emission), we infer that energy dissipation effects result in the lengthening of the calculated electron bubble expansion times by a numerical factor of ~2.0 for ^{4}He, ^{3}He, and Ne. Our theoretical result, $\tau_b^D = 8.5$ ps, for liquid ^{4}He at $P = 0$ is larger than the experimental estimate[33,34] of 2 ps for electron localization inferred from electron injection experiments. Of course, this experimental time scale for electron localization[33,34] does not reflect the properties of the equilibrated excess electron bubble and may correspond to a lower experimental time

limit for the electron bubble formation. The isotope effect $\tau_b^D(^4He)/\tau_b^D(^3He) = 0.83$ is invariant with respect to energy dissipation effects and reflects a balance between the effects of the equilibrium radii (Table 1) which increases τ_b^D in liquid ^{3}He relative to ^{4}He, in conjunction with density and surface tension effects which increase τ_b^D in ^{3}He. Of considerable interest are the predicted effects of the large electron bubble compressibility (with R_b shrinking from $R_b = 17$ Å for $p = 0$ to $R_b = 12$ Å at $p = 16$ atm[21,26]) on its bubble dynamics. From the data of Figure 3, we infer that the relative enhancement of the electron bubble formation time (τ_b^D/τ_b) due to dissipation effects is practically pressure independent. We predict the decrease of τ_b^D in liquid ^{4}He by a numerical factor of 4 in the range $p = 0$ to 20 atm (Figure 3), the major effects of the shortening of τ_b^D being due to the decrease of R_b at higher pressures (Figure 3). The details of the pressure dependence of the surface tension are not important for the calculation of τ_b^D at higher pressures, where the dominating contributions to $E_b(R)$, eq II.5, and to $\Delta E_D^{SE}(R)$, eq III.13, originate from the pressure−volume term. At $p = 16$ atm, we calculated $\tau_b^D = 2.12$ ps using the Amit−Gross formula[45] and $\tau_b^D = 2.09$ ps using the pressure independence value[24,46] $\gamma = 0.36$ dyn/cm.

The predicted electron bubble formation time in liquid Ne is considerably shorter than in liquid He, being predicted to be in the range of ∼1 ps. This prediction does not provide a clue for the existence of the two types of electrons in liquid Ne inferred from Muon spin-relaxation experiments with delocalized electrons, which do not relax on a time scale of 10^3 ps.[32]

V. Collapse Dynamics of an Empty Bubble

The dynamics of the expansion of the electron bubble radius from R_0 to R_b was found to be nearly exponential. The time (τ_b^D) for electron bubble expansion is considerably shorter than the collapse time (τ_c) for the collapse of the empty bubble (of initial radius R_b), which can be formed by the vertical photoionization of the electron bubble. In our previous work, we have applied the formula advanced by Lord Rayleigh to calculate the collapse time of the empty bubble in liquid ^{4}He, obtaining $\tau_c = 19.5$ ps.[37] Incorporating sound emission energy dissipation during the bubble contraction, τ_c is given by

$$\tau_c = (2\pi\rho)^{1/2}\int_{R_b}^{0} dR R^{3/2}[E_b(R_b) - E_b(R) - \Delta E_D^{SE}(R)]^{-1/2} \quad \text{(V.1)}$$

with $\Delta E_D^{SE}(R)$ being given by eq III.16 with $V_0 = 0$ and $E_e^{1s}(ER) = 0$ for all R. In Figure 4, we present the (nonexponential) time evolution of R (denoted as $R(f)$) during the collapse of the empty bubble in liquid ^{4}He and ^{3}He. As is apparent from Figure 4, the bubble collapse in liquid ^{4}He is faster than in ^{3}He. The time scales τ_c exhibit a marked isotope effect; i.e., $\tau_c = 19.8$ ps in ^{4}He and $\tau_c = 34$ ps in ^{3}He. The time scales for the empty bubble collapse are considerably longer than those for the electron bubble expansion, speeding it relative to the contraction of the empty bubble. The energy dissipation effects on the bubble collapse times are minor, with the difference between the $R(t)$ curves calculated without and with energy dissipation being about 2%. This behavior of the collapse of the empty bubble is in marked contrast with the substantial (100%) lengthening of τ_c for the expansion of the electron bubble (sections III and IV). Of course, the low velocity of the empty bubble collapse relative to the high velocity of the electron bubble expansion renders dissipation effects to be minor in the former case.

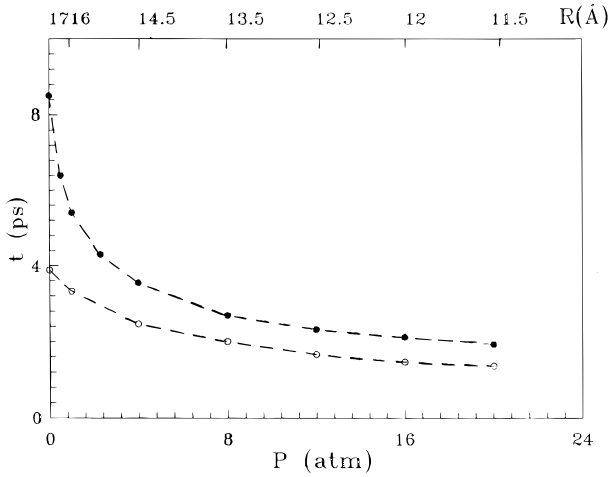

Figure 3. Pressure dependence ($P = 0-20$ atm) of the bubble expansion time in liquid ^{4}He τ_b. (○) Calculated in the absence of energy dissipation and of τ_b^D. (●) Calculated with dissipation due to sound emission. The equilibrium radii R_b of the electron bubble are also marked.

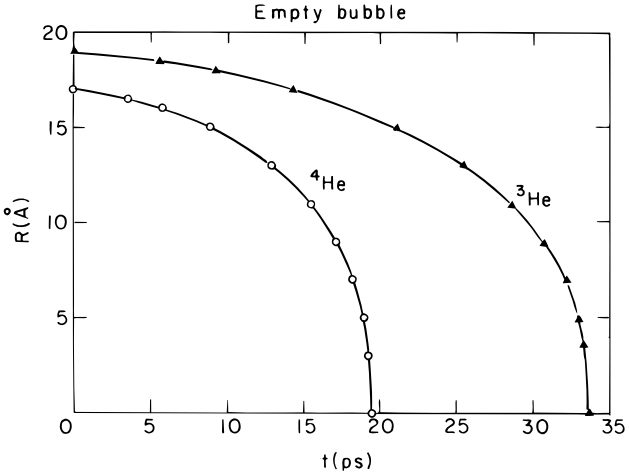

Figure 4. Dynamics of the collapse of an empty bubble in liquid ^{4}He (○) and in ^{3}He (▲) at $T = 0.4$ K, $P = 0$. The time dependence of the decrease of the radius R for the collapse of the empty bubble from R_b at $t = 0$ to $R = 0$ exhibits a marked isotope effect.

VI. Time-Resolved Electronic Spectroscopy

To make contact with real-life experiments, it is imperative to provide predictions for the interrogation of this new class of dynamic processes. Time-resolved electronic spectroscopy is expected to provide a powerful tool for the exploration of the time evolution of the electron bubble. The information on the time-resolved spectra was inferred from the potential energy surfaces (Figure 1) for the ground electronic 1s state, for the bound 1p and 2p excited electronic states, and for the quasifree electron state. These potential energy surfaces, in conjunction with the time-dependent radial configuration of the electron bubble (calculated incorporating energy dissipation effects), provide the input data for the calculation of the time-resolved electronic spectra. The time evolution of the bound−bound (1s → 1p and 1s → 2p) and of the bound−continuum (1s → V_0) electronic transitions will rest on the calculation of the time dependence of the energies of the corresponding vertical electronic transitions. To make contact with experimental reality for time-resolved electronic spectroscopy, one has to assume that the oscillator strengths for these electronic transitions exhibit a weak dependence on the electron bubble radius in the relevant bubble size domain. We shall subsequently show that this

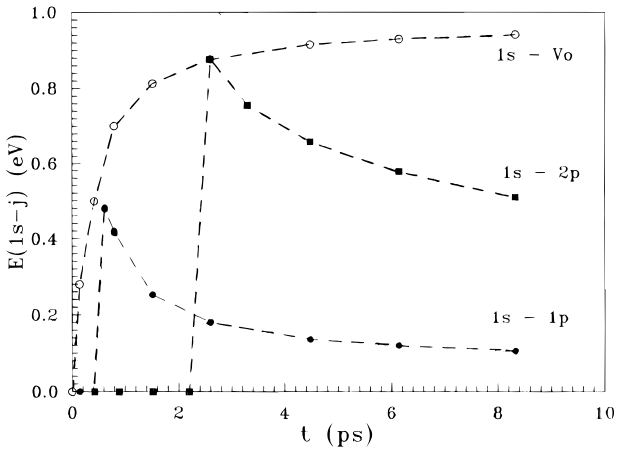

Figure 5. Time-resolved spectroscopy of the electron bubble in liquid ^{4}He. The time evolution of the vertical electronic transition energies for the bound−bound 1s → 1p (●) and 1s → 2p transitions (■) and for the bound−continuum 1s → V_0 vertical photoionization to the conduction band (○) are shown.

assumption is satisfied for the bound−bound electronic transitions.

The time dependence of the vertical ionization energy of the electron bubble from the 1s ground electronic state to the conduction band ($\Delta E_I(t)$) during the bubble expansion is presented in Figure 5 for liquid ^{4}He. The $\Delta E_I(t)$ vs t curve starts from low values at short times saturating at the asymptotic value of $\Delta E_I(\infty)$ for long times ($\Delta E_I(\infty) = 0.94$ eV for ^{4}He), which represents the vertical ionization potential of the electron bubble at its equilibrium configuration. The time evolution of $\Delta E_I(\infty)$ for liquid ^{4}He (Figure 5) can be well fit with a single exponential in the form $\Delta E_I(t) = \Delta E_I(\infty)(1 - ae^{-t/\tau})$ with the characteristic (kinetic time) of $\tau = 1.6$ ps.

Following the adiabatic expansion of the electron bubble in the ground electronic state, the allowed 1s → 1p and 1s → 2p electronic transitions will be exhibited (Figure 5). The time evolution of the absorption band maxima for the electronic spectra (Figure 5) exhibits an incubation time $t_{IN} = 1.2$ ps for the 1s → 1p and $t_{IN} = 3.3$ ps for the 1s → 2p transition. For $t > t_I$, the bound−bound (time-dependent) electronic spectrum will be amenable to experimental observation. The time-dependent peak energies ($\Delta E_{1s\rightarrow 1p}(t)$ and $\Delta E_{1s\rightarrow 2p}(t)$ of the 1s → 1p and 1s → 2p electronic spectra, respectively, decrease with time for both electronic transitions and converge to the equilibrium ($R = R_b$) excitation energies (Figure 5). These equilibrium peak energies are $\Delta E_{1s\rightarrow 1p}(\infty) = 0.11$ eV and $\Delta E_{1s\rightarrow 2p}(\infty) = 0.51$ eV. The time evolution of the excitation energies can be fit by a single-exponential function $\Delta E_{1s\rightarrow j}(t) - \Delta E_{1s\rightarrow j}(\infty) = b \exp(-1/\tau)$ (j = 1p, 2p) with $\tau = 2.0$ ps for the 1s → 1p and 1s → 2p transitions. The kinetic lifetime extracted from the time-resolved spectroscopy is only higher by 20% than the lifetime characterizing the time-resolved vertical ionization potential. This slight difference reflects the narrower R domain spanned by the bound−bound transitions.

These bound−bound electronic excitations are characterized by high oscillator strengths. For the equilibrium configuration ($R = R_b$), the oscillator strengths (calculated by numerical integration) are $f(1s\rightarrow 1p) = 0.93$ and $f(1s\rightarrow 2p) = 0.03$. The average oscillator strengths for the expanding electron bubble for $t = t_{IN}$ to τ_b were calculated to be $f^*(1s\rightarrow 1p) = 0.95$ and $f^*(1s\rightarrow 2p) = 0.04$. The small deviation between the equilibrium values of f and the dynamic values of f^* manifests a weak dependence of the oscillator strength for the bound−bound transitions on the configurational (R) of the electron bubble in the relevant R domain. This result will considerably simplify the analysis of time-resolved data, when these will become available.

Our theoretical predictions for the time-resolved electronic transitions provide the basis for the development of the experimental arsenal for the study of the temporal dynamics of electron localization in liquid He and Ne, which should be interrogated by ultrafast femtosecond laser spectroscopy.[50]

VII. Concluding Remarks

We have provided a description of localization dynamics of an excess electron in simple liquids, i.e., He and Ne, induced and accompanied by large configurational changes. Our treatment rests on a quantum mechanical Wigner−Seitz description of the excess electron in conjunction with a hydrodynamic picture for the liquid. Energy dissipation effects are of central importance to provide a realistic semiquantitative picture for the electron bubble dynamics. We have shown that the calculated electron bubble localization time is lengthened by about a numerical factor of 2 when energy dissipation due to the emission for sound waves is incorporated. We have shown[64] that the incorporation of energy dissipation due to viscosity effects has a small contribution and lengthens the τ_b^D data reported herein by only 10%. It should, however, be borne in mind that our treatment identifies the equilibrium bubble formation time with the first passage time of the bubble at $R = R_b$, with energy dissipation being averaged over the first period of the bubble's radial motion. This value of τ_b^D indeed represents the dominating time scale for the formation of the bubble, as reflected by the time dependence of the electronic energies. A more complete treatment should consider the expanding cavity radius overshooting R_b, exhibiting smell oscillations of the electron bubble radius around $R = R_b$, which will be damped by energy dissipation at $t > \tau_b^D$. These small oscillations in R will be manifested in the optical properties. We shall report on this problem in a subsequent publication.

The adiabatic electron bubble expansion can be envisioned as a dynamic solvation process of an excess electron in liquid He. In contrast to the solvation dynamics of an excess electron[51−53] of a giant dipole[54] in polar solvents, which is dominated by short-range short-time angular relaxation of the solvent molecules driven by inertial motion,[51−55] the electron bubble formation in liquid He and Ne involves a short-time radial expansion process. A more complete physical picture of excess electron solvation in simple monoatomic liquids involves a nonadiabatic electron-transfer process from the conduction band to the incipient bubble state, followed by the adiabatic expansion of the bubble. We have argued that the adiabatic expansion involves the dominant process, which determines the time scale for the formation of the equilibrated electron bubble ground electronic state. Nevertheless, the theoretical exploration of the truly ultrafast (fs) nonadiabatic initial electron localization from the conduction band to the incipient bubble state will be of interest.

Regarding the confrontation between the theoretical predictions and experimental reality, one has to consider the life story of an excess electron introduced (by a vertical optical excitation of the medium or of an electrode inserted in it) into the conduction band of the liquid. The relaxation process will involve the following steps: (a) energy relaxation; thermalization of the quasifree electron; (b) localization; the creation of the incipient bubble; (c) equilibration of the localized state of the adiabatic electron bubble expansion to its equilibrium configuration. We have focused herein on step c. Different experiments will interrogate different physical processes. In

this context, the distinction between ultrafast (subpicoseconds) localization (step b), which can be explored by electron injection, and equilibration of the localized state (step c), which can be interrogated by time-resolved ultrafast spectroscopy (section V), will be of considerable interest.

Acknowledgment. We are indeted to Dr. Ilya Rips for many stimulating discussions and for communicating to us the results of his work prior to publication. We are grateful to Professor A. G. Khrapak for useful information. This research was supported by the Deutsche Forschungsgemeinschaft (Sonderforschungsbereich 377).

References and Notes

(1) Kestner, N.; Jortner, J.; Cohen, M. H.; Rice, S. A. *Phys. Rev.* **1965**, *140*, A56.
(2) Rama Krishna, M. V.; Whaley, K. B. *Phys. Rev.* **1988**, *11*, 839.
(3) Space, B.; Coker, D.; Liu, Z.; Berne, B. J. *J. Chem. Phys.* **1992**, *97*, 2002.
(4) Springett, B. R.; Jortner, J.; Cohen, M. H. *J. Chem. Phys.* **1968**, *48*, 2720.
(5) (a) Jortner, J.; Kestner, N. R.; Cohen, M. H.; Rice, S. A. *J. Chem. Phys.* **1965**, *43*, 2614. (b) Hiroiki, K.; Kestner, N. R.; Rice, S. A.; Jortner, J. *J. Chem. Phys.* **1965**, *43*, 2625.
(6) Cheng, E.; Cole, M. W.; Cohen, M. H. *Phys. Rev. B* **1994**, *50*, 1136; *Phys. Rev. B* **1994**, *50*, 16134.
(7) Rosenblit, M.; Jortner, J. *J. Chem. Phys.* **1994**, *101*, 8039; *Phys. Rev. B* **1995**, *52*, 17461.
(8) Space, B.; Coker, D.; Liu, Z.; Berne, B. J.; Martyna, G. *J. Chem. Phys.* **1992**, *97*, 2002.
(9) Sommer, W. T. *Phys. Rev. Lett.* **1964**, *12*, 271.
(10) Woolf, M. A.; Rayfield, G. W. *Phys. Rev. Lett.* **1965**, *15*, 235.
(11) Broomall, J. R.; Johnson, W. D.; Onn, D. G. *Phys. Rev. B* **1976**, *14*, 2919.
(12) Plenkiewicz, B.; Plenkiewicz, P.; Jay-Garin, J. P. *Chem. Phys. Lett.* **1989**, *163*, 542.
(13) Martini, K.; Toennies, J. P.; Winkler, C. *Chem. Phys. Lett.* **1991**, *178*, 429.
(14) Jortner, J.; Gaathon, A. *Can. J. Chem.* **1977**, *53*, 1810.
(15) Schwenter, N.; Koch, E. E.; Jortner, J. *Electronic Excitations in Condensed Rare Gases*; Springer: Berlin, 1985.
(16) Cole, M. W. *Rev. Mod. Phys.* **1974**, *46*, 451.
(17) Edelman, V. S. *Sov. Phys. Usp.* **1980**, *23*, 227.
(18) Tauchert, W.; Jungblid, H.; Schmidt, W. F. *Can. J. Chem.* **1977**, *53*, 1860.
(19) Meyer, L.; Reif, F. *Phys. Rev.* **1960**, *119*, 1164.
(20) Fowler, W. B.; Dexter, D. L. *Phys. Rev.* **1976**, *176*, 337.
(21) Springett, B. E.; Cohen, M. H.; Jortner, J. *Phys. Rev.* **1967**, *159*, 183.
(22) Northby, J. A.; Sanders, T. M. *Phys. Rev. Lett.* **1967**, *18*, 1184.
(23) Miyakawa, T.; Dexter, D. L. *Phys. Rev. A* **1970**, *1*, 513.
(24) Grimes, C. C.; Adams, G. *Phys. Rev. B* **1990**, *41*, 6366; **1992**, *45*, 2305.
(25) Parshin, A. Ya.; Pereverzev, V. *Sov. Phys. JETP* **1992**, *74*, 68.
(26) Fetter, A. L. In *The Physics of Liquid and Solid Helium*; Bennerman, K. H., Ketterson, J. B., Eds.; Wiley: New York, 1976; pp 1, 207.
(27) Jiang, T.; Kim, C.; Northby, J. A. *Phys. Rev. Lett.* **1993**, *71*, 700.
(28) Northby, J. A.; Kim, C.; Jian, T. *Phys. B* **1994**, *197*, 426.
(29) Cohen, M. H.; Jortner, J. *Phys. Rev.* **1969**, *180*, 238.
(30) Ferrel, R. A. *Phys. Rev.* **1957**, *108*, 167.
(31) Briscoe, C. V.; Choi, S. I.; Stewart, A. T. *Phys. Rev. Lett.* **1968**, *20*, 493.
(32) Storchak, V.; Brewer, J. H.; Morris, G. D. *Phys. Rev. Lett.* **1996**, *76*, 2969.
(33) Hernandez, J. P.; Silver, M. *Phys. Rev. A* **1970**, *2*, 1949.
(34) Hernandez, J. P.; Silver, M. *Phys. Rev. A* **1971**, *3*, 2152.
(35) Jortner, J. *Ber. Bunseng. Phys. Chem.* **1971**, *75*, 696.
(36) Space, B.; Coker, D. F. *J. Chem. Phys.* **1991**, *94*, 1976; **1992**, *96*, 652.
(37) Rosenblit, M.; Jortner, J. *Phys. Rev. Lett.* **1995**, *75*, 4079.
(38) Stratt, J. W. (Lord Rayleigh) *Phil. Mag.* **1917**, *34*, 94.
(39) (a) Rips, I. *Chem. Phys. Lett.* **1995**, *245*, 79. (b) Rips, I. To be published.
(40) Khrapak, A. G. Private communication.
(41) Iakubov, I. T.; Khrapak, A. G. *Rep. Prog. Phys.* **1982**, *45*, 697.
(42) Artemev, A. A.; Khrapak, A. G. *Sov. Phys.-Tech. Phys. Lett.* **1986**, *12*, 1029.
(43) Schmidt, W. F.; Sakai, Y.; Khrapak, A. G. *Nucl. Inst. Methods Phys. Res. A.* **1993**, *327*, 87.
(44) Landau, L. D.; Lifschitz, E. M. *Fluid Mechanics*; Pergamon: Oxford, 1963.
(45) Amit, D.; Gross, E. P. *Phys. Rev.* **1966**, *145*, 130.
(46) Golov, A. *Z. Phys.* **1995**, *98*, 363.
(47) Shin, Y. M.; Woo, C.-W. *Phys. Rev. B* **1973**, *8*, 1437.
(48) Bersohn, R.; Zewail, A. H. *Ber. Bunsenges. Phys. Chem.* **1988**, *92*, 373.
(49) Jortner, J.; Levine, R. D. *Isr. J. Chem.* **1990**, *30*, 207.
(50) *Ultrafast Phenomena VIII*; Martin, J. L., Migus, A., Mourou, G. A., Zewail, A. H., Eds.; Springer Verlag: Berlin, 1993.
(51) Neria, E.; Nitzan, A.; Barnett, R. N.; Landman, U. *Phys. Rev. Lett.* **1991**, *67*, 1011.
(52) Migus, A.; Martin, J.; Antonetti, A. *Phys. Rev. Lett.* **1987**, *58*, 1559.
(53) Alfano, J.; Wallhout, P.; Kimura, Y.; Barbara, P. *J. Chem. Phys.* **1993**, *98*, 5996.
(54) Rosenthal, S. J.; Xie, X.; Du, M.; Fleming, G. R. *J. Chem. Phys.* **1991**, *95*, 4715.
(55) Rips, I.; Jortner, J. *J. Chem. Phys.* **1987**, *87*, 2090.
(56) Pandharipande, V. R.; Pieper, S. C.; Wiringa, R. B. *Phys. Rev. B* **1986**, *34*, 4571.
(57) Allen, J. F.; Misener, A. D. *Proc. Cambridge Phil. Soc.* **1938**, *34*, 299.
(58) Cole, M. W. *Phys. Rev. B* **1970**, *2*, 4239; **1971**, *3*, 4418.
(59) Kerr, E. C. *J. Chem. Phys.* **1957**, *26*, 511.
(60) Zinoveva, K. N. *Soviet Phys. JETP* **1955**, *2*, 774.
(61) Kerr, E. C. *Phys. Rev.* **1954**, *96*, 551.
(62) Van Urk, A. T.; Keesom, W. H.; Nijhoff, G. P. *Commun. Phys. Lab. Univ. Leiden* **1926**, *182b.*
(63) Mathias, E.; Crommelin, C. A.; Onnes, H. K. *Commun. Phys. Lab. Univ. Leiden* **1929**, *162b.*
(64) Rosenblit, M.; Jortner, J. To be published.